NANO LETTERS

Letter

pubs.acs.org/NanoLett

Super-Resolution Microscopy Using Standard Fluorescent Proteins in Intact Cells under Cryo-Conditions

Rainer Kaufmann,[†,‡] Pascale Schellenberger,[†] Elena Seiradake,[†] Ian M. Dobbie,[‡] E. Yvonne Jones,[†] Ilan Davis,[‡] Christoph Hagen,[†] and Kay Grünewald*[,†]

[†]Division of Structural Biology, Wellcome Trust Centre for Human Genetics and [‡]Department of Biochemistry, University of Oxford, Oxford, United Kingdom

Supporting Information

ABSTRACT: We introduce a super-resolution technique for fluorescence cryo-microscopy based on photoswitching of standard genetically encoded fluorescent marker proteins in intact mammalian cells at low temperature (81 K). Given the limit imposed by the lack of cryo-immersion objectives, current applications of fluorescence cryo-microscopy to biological specimens achieve resolutions between 400−500 nm only. We demonstrate that the single molecule characteristics of reversible photobleaching of mEGFP and mVenus at liquid nitrogen temperature are suitable for the basic concept of single molecule localization microscopy. This enabled us to perform super-resolution imaging of vitrified biological samples and to visualize structures in unperturbed fast frozen cells for the first time with a structural resolution of ∼125 nm (average single molecule localization accuracy ∼40 nm), corresponding to a 3−5 fold resolution improvement.

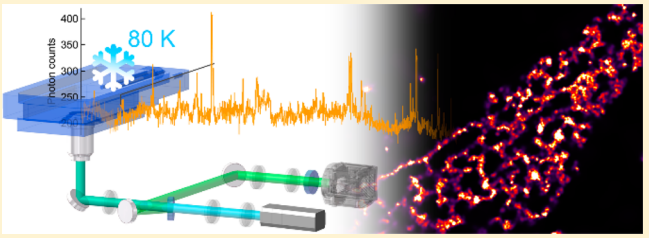

KEYWORDS: *Fluorescence cryo-microscopy, vitrification, localization microscopy, single molecule blinking, low temperature, frozen-hydrated cells*

To study the fine details of biological structures with microscopy, both the preservation of these structures during the preparation process and the achievable resolution of the imaging system are of equal importance.[1] In the field of fluorescence microscopy, the latter has been addressed by various super-resolution methods that have been developed in recent years to overcome the diffraction-limited resolution of light microscopy. These include STED (stimulated emission depletion microscopy),[2] SIM (structured illumination microscopy),[3,4] PALM (photo-activated localization microscopy),[5] FPALM (fluorescence photoactivation localization microscopy),[6] and STORM (stochastic optical reconstruction microscopy).[7] To ensure best preservation of biological structures, ultimately super-resolution imaging should be performed in living cells, but this remains very challenging.[8−10] Typically, chemical fixation of the samples to immobilize the structures of interest is required to achieve the best technical results, but unfortunately, this is associated with structural changes in the sample,[11] especially at a size range that is relevant for light microscopic techniques achieving resolutions below the diffraction limit.[12] A preferable alternative is vitrification (i.e., cryo-immobilizing the structure in glasslike amorphous ice using rapid freezing techniques) that preserves the structures in a near-native state and is frequently used in the fields of electron and X-ray cryo-microscopy.[13,14]

The advantages of vitrified specimens have not been fully exploited to date in fluorescence microscopy of subcellular structures. This is because one of the biggest challenges for imaging vitrified biological samples with fluorescence cryo-microscopy is currently limited resolution due to the inherent technical challenges of the setup[15] and in particular the lack of commercially available high NA cryo-immersion objectives.[16] For systems operated at low temperatures, the reduced resolution and imaging quality due to low NA objectives generally present obstacles for imaging but also for spectroscopic applications.[17−20] The feasibility of immersing an objective with an NA of 1.3 for fluorescence imaging under cryo-conditions has been demonstrated in principle;[19] however, the effective NA of the system and possible aberrations introduced by refractive index mismatches[21] has not been characterized. It currently remains unknown to what extent the potentially higher achievable resolution of existing water or oil immersion objectives will be compromised under cryo-conditions by introducing aberrations due to different thermal expansion coefficients of different elements in the objective. Therefore, previous publications on vitrified cellular samples reported a resolution with best values in the range of 400−500 nm measured with different fluorescence cryo-microscopy implementations.[15,16,22] These were all basic wide-field setups, and no successful super-resolution cryo-microscopy of biological specimens has yet been reported.

Most of the super-resolution methods developed for fluorescence imaging at ambient temperature are based on

Received: May 20, 2014
Published: June 2, 2014

   dx.doi.org/10.1021/nl501870p | *Nano Lett.* 2014, 14, 4171−4175

the ability of the fluorophore to be switched between a bright and a dark state.[23] For isolated organic dye molecules, single molecule blinking at low temperature (4 K) has been observed in previous studies with lifetimes of the bright state (τ_b) of the fluorescent molecules similar to the lifetime of the dark state (τ_d).[24,25] Using a priori information about the object, precise distance measurements in the nanometer range were performed, however, super-resolution imaging was not demonstrated.[25] Fluorescent proteins also have been shown to undergo reversible photobleaching at low temperatures (both 1.6 and 100 K).[26,27] Moderate to high excitation intensities (kW/cm^2 range) switch a subset of the molecules to a reversibly bleached state from which the recovery to the fluorescent state occurs spontaneously or can be photo-induced.[26,27] Photoswitching of standard genetically encoded fluorescent proteins at low temperatures is facilitated by photoinduced protonation rather than conformational changes such as isomerization that play a competing role at ambient temperatures.[27] So far, this has been characterized only in bulk studies, thus not allowing insights into the photophysics of the switching at the single molecule level and a more detailed understanding of the different pathways of reversible and irreversible photobleaching of standard fluorescent proteins at low temperatures.

In this study, we show that at ~80 K the lifetimes of τ_b and τ_d of individual standard fluorescent proteins in a three-dimensional and crowded cellular environment are suitable for the basic concept of single molecule localization microscopy (SMLM; $\tau_b \ll \tau_d$). We utilize the stochastic recovery from the dark state for high-accuracy localization of single molecule positions for super-resolution imaging of vitrified biological samples at low temperatures and describe the implementation of this technique. This approach allowed us to overcome the diffraction limit in fluorescence cryo-microscopy. Single molecule blinking of standard fluorescent marker proteins in vitrified cells allowed us to determine their positions with high precision (10−50 nm range) and the visualization of biological structures with a resolution of 100−150 nm at liquid nitrogen temperature (Figures 1 and 2). This corresponds to a 3−5 fold improvement in resolution compared to previous achievements in the field of fluorescence cryo-microscopy and lies well within the definition of super-resolution.[28]

We performed the measurements with the Cryostage2[29] operated with liquid nitrogen cooling and in conjunction with a long working distance air objective incorporated in a custom built wide-field setup (Figure 3, for details see Supporting Information S1.3). The objective's NA of 0.75 limits the optical resolution of the setup to ~450 nm due to diffraction. The mechanical stability of the setup is another vital aspect to consider for advanced fluorescence cryo-microscopy. We were able to keep the temperature inside the cryo-stage constant at 81 K over the course of the measurements. This is crucial for preventing the sample from drifting, especially in the axial direction, that is, out of focus. We likewise succeeded in reducing instabilities in the lateral plane to amplitudes in the 50−100 nm range (Figure 3). Tracking of endogenous bright objects in the background (here strongly fluorescent fluorophore aggregates; alternatively, fiducial markers can be used) allowed us to measure these instabilities during the data collection for cryo-SMLM (see Supporting Information S1.5). This procedure allowed us to calculate the extent of the drift, which we then used to correct the determined single molecule positions. Much larger lateral instabilities (μm range) can be corrected this way for achieving a super-resolution image under less stable conditions (Supporting Information Figure S1).

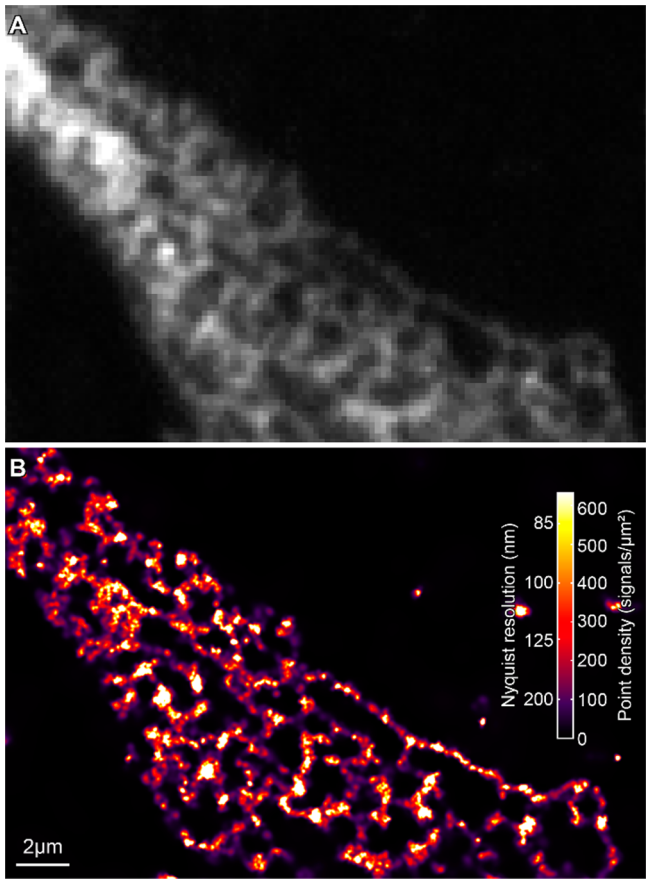

Figure 1. Single molecule super-resolution cryo-imaging. (A) Wide-field fluorescence cryo-microscopy image of endoplasmic reticulum labeled with mVenus in a vitrified cell. Resolution: ~450 nm. (B) Corresponding cryo super-resolution image of single molecule localization cryo-microscopy. Average localization accuracy: 42 nm. Structural resolution: ~125 nm. Color coding indicates local densities of detected single molecule positions as well as the corresponding Nyquist resolution.

The illumination intensity has to be adjusted to enable the photoinduced switching of standard fluorescent proteins. We used an excitation laser with a wavelength of 488 nm and intensities in the range of 1−2 kW/cm^2 for cryo-SMLM imaging of mVenus and mEGFP labeled membrane structures (see Supporting Information S1.1, S1.2). Typically, 6000−10 000 images were recorded with an EMCCD camera at a frame rate of 20 fps (36 ms integration time, 14 ms readout time per frame). For the case described here, where the numbers of detectable photons are limited due to the objective's NA of 0.75, it is of particular importance to have high sensitivity detectors and to match the detector integration times with the periods τ_b that the fluorescent proteins remain in the bright state. The average number of photons detected per pixel in a 3 × 3 region of interest (ROI) over the course of 100 s (Figure 2C) illustrates the typical stochastic recovery of single molecules from the reversibly bleached state during the localization microscopy measurement at low temperature. τ_b was in the range of 10−100 ms whereas the lifetime τ_d of the reversible dark state lasted for many seconds up to minutes. This enabled the separation of single molecule signals originating from the densely packed standard fluorescent

dx.doi.org/10.1021/nl501870p | Nano Lett. 2014, 14, 4171−4175

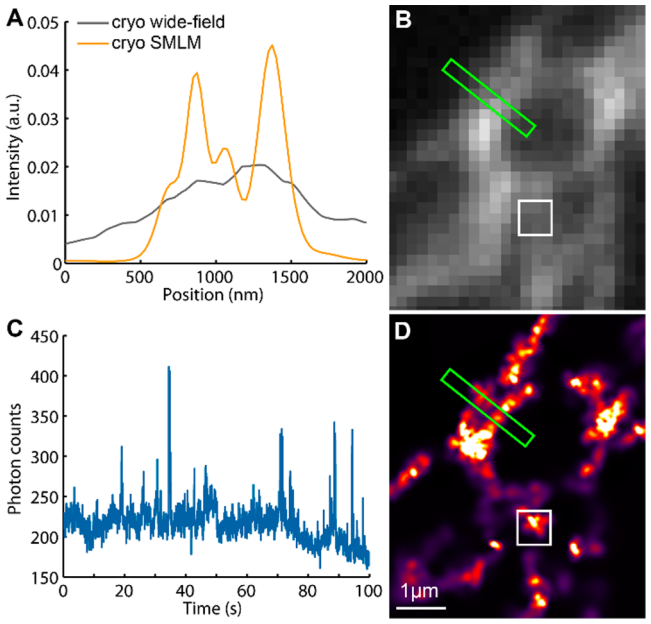

Figure 2. Characterization of single molecule localization cryo-microscopy (cryo-SMLM) imaging. (A) Normalized intensity profiles along a line indicated by the green rectangles (line width: 250 nm) in (B) (wide-field image) and (D) (super-resolution cryo-microscopy image, same color code as in Figure 1B applies) of membrane structures labeled with mVenus. (C) Average number of detected photons per pixel in a 3 × 3 ROI over 2000 frames of the raw data stack used in (D) in the area indicated by the white squares in (B,D). Fluorescence bursts of single molecules recovering from the reversibly bleached state are clearly visible above the relatively high background noise.

protein labeling of the biological structures. The attained average single molecule localization accuracy of ∼40 nm at ∼80 K is approximately a factor of 2 lower than the typically achieved values with oil immersion objective lenses at ambient temperatures. This corresponds to what would be expected by the difference of the objectives NAs and therefore indicates that the number of emitted photons of the fluorescent proteins per switching cycle shows no strong temperature dependency. A similar behavior has been observed previously for organic dye molecules at liquid helium temperature (4 K)[24] where the number of detected photons per switching cycle was similar to other studies performed at ambient temperatures.[30]

Our concept of data collection and image formation here is analogous to what has been shown for SMLM of standard fluorescent proteins at ambient temperatures.[31−33] For the determination of the single molecule positions, we used an algorithm that is able to handle raw data with a high background.[34] We slightly modified the algorithm to adapt it to our setup and imaging conditions (see Supporting Information S1.4). Background fluorescence in cellular samples arises from out of focus information due to the three-dimensional extension of the structures but also from endogenous autofluorescent molecules of the cell that are more resistant to bleaching under cryo-conditions as compared to ambient temperatures. Figures 1 and 2 show the results of super-resolution cryo-imaging of mVenus labeled endoplasmic reticulum (ER) in vitrified COS7 cells. The average single molecule localization accuracy was ∼40 nm; the achieved structural resolution was ∼125 nm (see Supporting Information S1.6). The intensity profiles of the membrane structures in Figure 2 clearly reveal the improvement in observable details compared to the basic wide-field cryo-image with a resolution of ∼450 nm.

The results we report here show that the level of resolution achieved by the introduction of cryo-SMLM already reaches the capabilities of certain other super-resolution techniques at ambient temperatures, such as SIM. However, to attain this SIM necessarily depends on using oil immersion objective lenses with an NA of at least 1.2.[9,35] High NA objectives are so far not available for fluorescence cryo-microscopy, but the achievable resolution in single molecule super-resolution cryo-microscopy would greatly benefit from the development of cryo-immersion objectives. As the localization accuracy σ is mainly dependent on the standard deviation of the point spread function (PSF) s and the number of detected photons N,

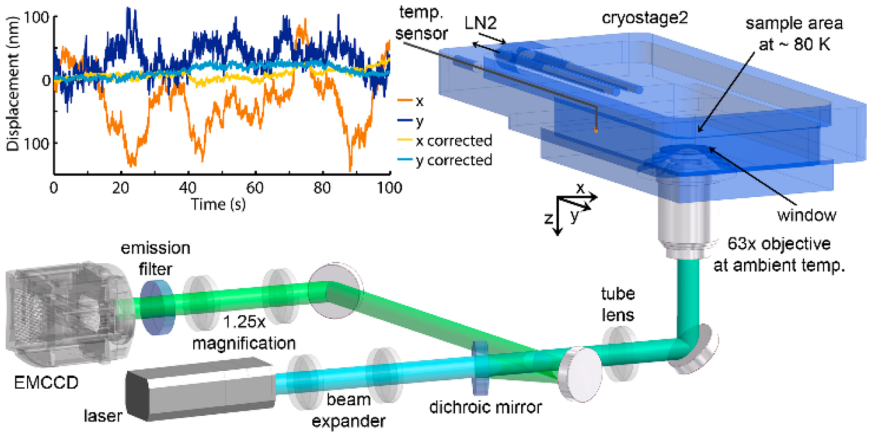

Figure 3. Schematic drawing of the cryo-SMLM setup. Excitation and detection path of the setup are conventional wide-field configurations (for more details see Supporting Information S1.3). The long working distance air objective is kept at ambient temperature and is separated from the cryo-environment inside the cryo-stage by a glass window of standard coverslip thickness. The temperature in the sample area is controlled by a pump regulating the liquid nitrogen flow into the cryo-stage with a feedback loop of a temperature sensor placed inside (for more details regarding the Cryostage2, see Rigort et al.[29]). The graph shows the lateral stability of the sample in the cryo-stage over a time of 100 s. The light blue and yellow lines represent the stability after correction based on tracking of bright features in the background in the individual frames with respect to the first frame during localization microscopy imaging.

dx.doi.org/10.1021/nl501870p | Nano Lett. 2014, 14, 4171−4175

($\sigma \sim s/\sqrt{N}$), an improvement of more than 2-fold is expected as result of an NA increase to above 1.2 (from the current NA of 0.75). The significantly better signal-to-noise ratio would likewise increase the detection efficiency and thereby the Nyquist limited resolution. A higher NA would also be hugely beneficial for 3D single molecule localization as the width of the PSF in the axial direction is proportional to NA^{-2}. For increased localization accuracies and high NA objectives, the dipole moment of fluorophores that are fixed or at least hindered in their orientation will have to be considered.[36,37] For the combination of higher NA with detection through media with a larger refractive index (n = 1.5) it has been shown that localization errors can reach values up to ~13 nm.[25] For objectives with an NA of <1.0 and detection through a medium with low refractive index (n = 1.0), this effect is in the range of a few angstroms and can be neglected.[25]

Using standard genetically encoded fluorescent proteins for single molecule super-resolution cryo-microscopy is highly beneficial from several points of views. Compared to special photoswitchable or photoactivatable fluorophores, cryo-SMLM using standard fluorescent proteins allows for a significantly wider range of biological applications. For the study of intracellular structures immobilized in their most native state, the combination of endogenous fluorescent protein markers, vitrification of the specimen, and imaging under cryo-conditions will provide best results. More importantly, the use of organic dye molecules introduces the fundamental complication of labeling intracellular structures in living, nonpermeabilized cells that typically results in perturbing the specimen before vitrification for fluorescence cryo-microscopy. However, for proteins or molecules on exposed cellular surfaces or noncellular samples (e.g., virus particles), organic dyes might be advantageous because of the higher photon yield per switching cycle compared to fluorescent proteins (studied at ambient temperature[30]). It has been observed that photo-decomposition of fluorescent molecules, greatly reduced at low temperature,[38] in general can be used to improve the localization accuracy of isolated single molecules dramatically.[25] However, in cellular samples the autofluorescence of endogenous molecules is also stabilized leading to a higher and much slower bleaching background as compared to conditions at ambient temperatures. In the case of three-dimensionally extended structures, out-of-focus light additionally reduces the signal-to-noise ratio for single molecule detection, as so far, due to the lack of high NA immersion objectives, no optical sectioning such as TIRF (total internal reflection fluorescence) microscopy has been successfully applied under cryo-conditions. The development of dedicated genetically encodable fluorophores to exploit the specific photophysics under cryo-conditions, the optimization of the fluorophore microenvironment, or the use of imaging conditions that provide a slowed-down switching cycle (longer lifetimes of bright and dark state with $\tau_b \ll \tau_d$) may open ways to further increase the resolution of cryo-SMLM. Both (i) reaching a higher photon yield per single molecule blinking event while still keeping them separable from each other to increase the single molecule localization accuracy and (ii) optimizing the switching efficiency of the fluorescent molecules at low temperatures (on which the achievable Nyquist limited resolution is fundamentally dependent) are of equal importance for super-resolution cryo-imaging.

In summary, we have demonstrated that cryo-SMLM in vitrified cellular samples using standard fluorescent proteins improves the resolution in fluorescence cryo-microscopy to far below the diffraction limit. The combination of a sufficiently stable cryo-stage equipped with a sample transfer mechanism, drift correction, and an algorithm for single molecule localization of signals with high background allowed us to investigate at a temperature of ~80 K single molecule blinking of standard fluorescent proteins and to successfully establish super-resolution fluorescence imaging of genuine structures inside vitrified cells. On the basis of these results, we expect that super-resolution cryo-microscopy will become a valuable imaging method for cryo-immobilized biological samples that is highly complementary to electron and X-ray cryo-microscopy for the study of cellular and subcellular complexity. Technical advances such as the development of immersion cryo-objectives will improve the achievable resolution further, potentially to even beyond what has been shown for SMLM at ambient temperatures, and turn fluorescence cryo-microscopy into a powerful technique for imaging cellular structures in a near-native state at nanometer resolution.

■ ASSOCIATED CONTENT

Ⓢ Supporting Information

Detailed description of materials and methods, including sample preparation, optical setup, cryo-SMLM imaging, data analysis, drift correction, and resolution assessment; figures depicting results of mEGFP, drift correction, and additional parameter filtering for cryo-SMLM data. This material is available free of charge via the Internet at http://pubs.acs.org.

■ AUTHOR INFORMATION

Corresponding Author

*E-mail: kay@strubi.ox.ac.uk.

Notes

The authors declare no competing financial interest.

■ ACKNOWLEDGMENTS

We are grateful to Miriam Stoeber and Ari Helenius (Zurich) for generous gifts of plasmid CAV1-mEFGP and Jordan Raff and Daven Vasishtan (Oxford) for constructive discussion and critical reading of the manuscript. This work was supported by Wellcome Trust Senior Research Fellowships (090895/Z/09/Z to K.G. and 096144/Z/11/Z to I.D.), the Wellcome Trust core award to the Wellcome Trust Centre for Human Genetics (090532/Z/09/Z), an EMBO Fellowship (ALTF 642-2011 to P.S.) a Cancer Research UK programme grant (A10976 to E.Y.J.) and the Micron Strategic Award from the Wellcome Trust (091911).

■ REFERENCES

(1) Leis, A.; Rockel, B.; Andrees, L.; Baumeister, W. *Trends Biochem. Sci.* **2009**, *34* (2), 60−70.
(2) Hell, S. W.; Wichmann, J. *Opt. Lett.* **1994**, *19* (11), 780−782.
(3) Heintzmann, R.; Cremer, C. *Proc. Soc. Photo-Opt. Instrum. Eng.* **1999**, *3568*, 185−196.
(4) Gustafsson, M. G. L. *J. Microsc.* **2000**, *198*, 82−87.
(5) Betzig, E.; Patterson, G. H.; Sougrat, R.; Lindwasser, O. W.; Olenych, S.; Bonifacino, J. S.; Davidson, M. W.; Lippincott-Schwartz, J.; Hess, H. F. *Science* **2006**, *313* (5793), 1642−1645.
(6) Hess, S. T.; Girirajan, T. P. K.; Mason, M. D. *Biophys. J.* **2006**, *91* (11), 4258−4272.
(7) Rust, M. J.; Bates, M.; Zhuang, X. W. *Nat. Methods* **2006**, *3* (10), 793−795.
(8) Westphal, V.; Rizzoli, S. O.; Lauterbach, M. A.; Kamin, D.; Jahn, R.; Hell, S. W. *Science* **2008**, *320* (5873), 246−249.

(9) Shao, L.; Kner, P.; Rego, E. H.; Gustafsson, M. G. L. *Nat. Methods* **2011**, *8* (12), 1044−1046.
(10) Jones, S. A.; Shim, S. H.; He, J.; Zhuang, X. W. *Nat. Methods* **2011**, *8* (6), 499−505.
(11) Bleck, C. K. E.; Merz, A.; Gutierrez, M. G.; Walther, P.; Dubochet, J.; Zuber, B.; Griffiths, G. *J. Microsc.* **2010**, *237* (1), 23−38.
(12) Weinhausen, B.; Saldanha, O.; Wilke, R. N.; Dammann, C.; Priebe, M.; Burghammer, M.; Sprung, M.; Köster, S. *Phys. Rev. Lett.* **2014**, *112* (8), 088102.
(13) Hurbain, I.; Sachse, M. *Biol. Cell* **2011**, *103* (9), 405−420.
(14) Schneider, G.; Guttmann, P.; Rehbein, S.; Werner, S.; Follath, R. *J. Struct. Biol.* **2012**, *177* (2), 212−223.
(15) Briegel, A.; Chen, S.; Koster, A. J.; Plitzko, J. M.; Schwartz, C. L.; Jensen, G. J. *Methods Enzymol.* **2010**, *481*, 317−341.
(16) Schellenberger, P.; Kaufmann, R.; Siebert, C. A.; Hagen, C.; Wodrich, H.; Grünewald, K. *Ultramicroscopy* **2013**, *143*, 41−51.
(17) Schwartz, C. L.; Sarbash, V. I.; Ataullakhanov, F. I.; McIntosh, J. R.; Nicastro, D. *J. Microsc.* **2007**, *227* (Pt 2), 98−109.
(18) Sartori, A.; Gatz, R.; Beck, F.; Rigort, A.; Baumeister, W.; Plitzko, J. M. *J. Struct. Biol.* **2007**, *160* (2), 135−145.
(19) Le Gros, M. A.; McDermott, G.; Uchida, M.; Knoechel, C. G.; Larabell, C. A. *J. Microsc.* **2009**, *235* (1), 1−8.
(20) Hussels, M.; Konrad, A.; Brecht, M. *Rev. Sci. Instrum.* **2012**, *83* (12), 123706.
(21) Hell, S.; Reiner, G.; Cremer, C.; Stelzer, E. H. K. *J. Microsc.* **1993**, *169*, 391−405.
(22) van Driel, L. F.; Valentijn, J. A.; Valentijn, K. M.; Koning, R. I.; Koster, A. J. *Eur. J. Cell Biol.* **2009**, *88* (11), 669−684.
(23) Hell, S. W. *Nat. Methods* **2009**, *6* (1), 24−32.
(24) Weisenburger, S.; Jing, B.; Renn, A.; Sandoghdar, V. *Proc. SPIE* **2013**, *8815*, 88150D-1.
(25) Weisenburger, S.; Jing, B.; Hänni, D.; Reymond, L.; Schuler, B.; Renn, A.; Sandoghdar, V. *ChemPhysChem* **2014**, *15* (4), 763−770.
(26) Creemers, T. M.; Lock, A. J.; Subramaniam, V.; Jovin, T. M.; Volker, S. *Proc. Natl. Acad. Sci. U.S.A.* **2000**, *97* (7), 2974−2978.
(27) Faro, A. R.; Adam, V.; Carpentier, P.; Darnault, C.; Bourgeois, D.; de Rosny, E. *Photochem. Photobiol. Sci.* **2010**, *9* (2), 254−262.
(28) Galbraith, C. G.; Galbraith, J. A. *J. Cell Sci.* **2011**, *124* (10), 1607−1611.
(29) Rigort, A.; Bäuerlein, F. J.; Leis, A.; Gruska, M.; Hoffmann, C.; Laugks, T.; Böhm, U.; Eibauer, M.; Gnaegi, H.; Baumeister, W.; Plitzko, J. M. *J. Struct. Biol.* **2010**, *172* (2), 169−179.
(30) Dempsey, G. T.; Vaughan, J. C.; Chen, K. H.; Bates, M.; Zhuang, X. *Nat. Methods* **2011**, *8* (12), 1027−1036.
(31) Lemmer, P.; Gunkel, M.; Baddeley, D.; Kaufmann, R.; Urich, A.; Weiland, Y.; Reymann, J.; Müller, P.; Hausmann, M.; Cremer, C. *Appl. Phys. B: Laser Opt.* **2008**, *93* (1), 1−12.
(32) Biteen, J. S.; Thompson, M. A.; Tselentis, N. K.; Bowman, G. R.; Shapiro, L.; Moerner, W. E. *Nat. Methods* **2008**, *5* (11), 947−949.
(33) Fölling, J.; Bossi, M.; Bock, H.; Medda, R.; Wurm, C. A.; Hein, B.; Jakobs, S.; Eggeling, C.; Hell, S. W. *Nat. Methods* **2008**, *5* (11), 943−945.
(34) Grüll, F.; Kirchgessner, M.; Kaufmann, R.; Hausmann, M.; Kebschull, U. *IEEE Int. Conf. Field. Prog. Logic Appl.* **2011**, *21*, 1−5.
(35) Schermelleh, L.; Carlton, P. M.; Haase, S.; Shao, L.; Winoto, L.; Kner, P.; Burke, B.; Cardoso, M. C.; Agard, D. A.; Gustafsson, M. G.; Leonhardt, H.; Sedat, J. W. *Science* **2008**, *320* (5881), 1332−1336.
(36) Engelhardt, J.; Keller, J.; Hoyer, P.; Reuss, M.; Staudt, T.; Hell, S. W. *Nano Lett.* **2011**, *11* (1), 209−213.
(37) Lew, M. D.; Backlund, M. P.; Moerner, W. E. *Nano Lett.* **2013**, *13* (9), 3967−3972.
(38) Moerner, W. E.; Orrit, M. *Science* **1999**, *283* (5408), 1670−1676.